Available online at www.sciencedirect.com
ScienceDirect
Computers and Chemical Engineering 32 (2008) 1257–1269
Computers & Chemical Engineering
www.elsevier.com/locate/compchemeng

Stochastic-based accuracy of data reconciliation estimators for linear systems

Miguel J. Bagajewicz *, DuyQuang Nguyen

University of Oklahoma, 100 E. Boyd St., T-335, Norman, OK 73019, United States

Received 28 June 2006; received in revised form 31 May 2007; accepted 4 June 2007
Available online 26 June 2007

Abstract

Accuracy of an instrument has been traditionally defined as the sum of the precision and the bias. Recently, this notion was generalized to estimators [Bagajewicz, M. (2005a). On the definition of software accuracy in redundant measurement systems. *AIChE Journal*, *51*(4), 1201–1206]. The definition was based on the maximum undetected bias and ignored the frequency of failure, thus providing an upper bound. In more recent work [Bagajewicz, M. (2005b). On a new definition of a stochastic-based accuracy concept of data reconciliation-based estimators. In *European Symposium on Computer-Aided Process Engineering Proceeding (ESCAPE)*], a more realistic concept of expected value of accuracy was presented. However, only the timing of failure and the condition of failure was sampled. In this paper we extend the Monte Carlo simulations to also sample the size of the gross errors and we provide new insights on the evolution of biases through time.

Keywords: Instrumentation; Accuracy

1. Introduction

Traditionally, accuracy of an instrument is defined as the sum of the precision and the bias (Miller, 1996). Recently, this notion was generalized to estimators (Bagajewicz, 2005a), arguing that the accuracy of an estimator is the sum of the precision and the maximum induced bias. This maximum induced is the maximum value of the bias of the estimator in question, which is a result of a certain specific number of biases in the network. The concept also makes use of an underlying assumption about the technique to detect biases. To illustrate the concept, Bagajewicz (2005a) used a serial elimination technique based on the maximum power measurement test (MPMT). However, he ignored the frequency of failures, in fact referring to a static situation ignoring temporal averages. To ameliorate this deficiency, in a recent conference paper (Bagajewicz, 2005b) the definition of accuracy was modified to include expected undetected biases (as opposed to maximum values) and their frequency. The paper used Monte Carlo simulations to assess the value of accuracy but it only sampled the time of the failure and the condition of the failure (detected or undetected). It did not sample over the size of the error, thus making assumptions about detectability that are weak.

In this paper, bias size and evolution in time are also considered and sampled and other properties of accuracy as a function of time are explored.

2. Background

Accuracy has been defined as precision (standard deviation) plus absolute value of systematic bias (Miller, 1996). However, this definition is of little practical use unless the systematic bias can be independently determined. If biases are present somewhere in the system and they are too small to be detected, they smear all the estimators, including those of the variables for which the corresponding instruments have no bias, called induced bias. The vector of induced biases ($\hat{\boldsymbol{\delta}}$) is defined as the difference between the vector of expected values of the estimators $\widehat{\boldsymbol{x}}$ when gross errors are present and the vector of true values of process variables ($\boldsymbol{x}$) of (Bagajewicz, 2005a, 2005b):

$$\hat{\boldsymbol{\delta}} = E[\widehat{\boldsymbol{x}}] - \boldsymbol{x} = [\boldsymbol{I} - \boldsymbol{SW}]\boldsymbol{\delta} \tag{1}$$

where $\boldsymbol{I}$ is the identity matrix, $\boldsymbol{S}$ the variance matrix of measurements, $\boldsymbol{\delta}$ the actual biases in measurements and $\boldsymbol{W} = \boldsymbol{A}^{\mathrm{T}}(\boldsymbol{ASA}^{\mathrm{T}})^{-1}\boldsymbol{A}$, where $\boldsymbol{A}$ is process constraints matrix.

* Corresponding author.
E-mail address: bagajewicz@ou.edu (M.J. Bagajewicz).

0098-1354/$ – see front matter © 2007 Elsevier Ltd. All rights reserved.
doi:10.1016/j.compchemeng.2007.06.016

Nomenclature

$a_{i,(t_s,t_{s+1})}$	accuracy value of estimator i within a time interval (t_s, t_{s+1})
$\hat{a}_i$	accuracy of estimator i
$\bar{a}_i$	average value of accuracy of estimator i
$\boldsymbol{A}$	process constraints matrix
$E[\hat{a}_i]$	expected value of accuracy of estimator i
$h_k(\theta_k, \bar{\delta}_k, \rho_k)$	probability distribution function of bias k with mean $\bar{\delta}_k$ and standard deviation ρ_k
$\boldsymbol{S}$	variance matrix of measurements
$\hat{\boldsymbol{S}}$	variance matrix of the estimators
T_h	time horizon
$\boldsymbol{x}$	true values of process variables
$\widehat{\boldsymbol{x}}$	estimators of process variables
$Z^{\mathrm{MP}}_{d,j}$	maximum power measurement test statistic for measurement j

Greek letters

$\boldsymbol{\delta}$	actual biases
$\boldsymbol{\delta}_{n_T}$	sizes of set T of n_T undetected biases
$\hat{\boldsymbol{\delta}}$	induced biases
δ^*_i	maximum undetected induced bias in estimator i
$\tilde{\delta}^{(p,n_T)}_i$	induced bias in estimator i due to a specific set T of n_T undetected biases at confidence level p
$\hat{\sigma}_i$	precision of estimator i
$\hat{\sigma}^{\mathrm{R}}_i$	residual precision of estimator i

Then accuracy is defined as the sum of precision plus the maximum possible undetected induced bias in the estimator i (Bagajewicz, 2005a):

$$\hat{a}_i = \hat{\sigma}_i + \delta^*_i \tag{2}$$

where $\hat{a}_i$, $\hat{\sigma}_i$, δ^*_i are the accuracy, precision (square root of variance S_{ii}) and the maximum undetected induced bias of the estimator i, respectively.

By definition, the accuracy value relies on how one calculates the induced bias. Because the induced bias in the estimator is based on undetected biases whose sizes can be any value below the threshold detection values and their location can be anywhere in the system, the induced bias is a random number. Bagajewicz (2005a) proposed to calculate accuracy as the sum of precision and the maximum possible value of undetected induced bias. However, one can also calculate the induced bias as the expected value of all possible values. The latter is a more realistic approach. The accuracy value also depends on the technique to detect gross errors. In this work, we use the maximum power measurement test (MPMT) to detect gross errors because of its popularity and simple calculation procedure. The MPMT is briefly described below.

The measurement test (MT) is based on the vector of measurement adjustments $\boldsymbol{m}$:

$$\boldsymbol{m} = \boldsymbol{y} - \widehat{\boldsymbol{x}} = \boldsymbol{S}\boldsymbol{A}^{\mathrm{T}}(\boldsymbol{A}\boldsymbol{S}\boldsymbol{A}^{\mathrm{T}})^{-1}\boldsymbol{A}\boldsymbol{y} \tag{3}$$

where $\boldsymbol{y}$ is the vector of measurements and $\widehat{\boldsymbol{x}}$ are reconciled estimators of the process variables. The maximum power (MP) measurement test proposed by Mah and Tamhane (1982) is based on vector $\boldsymbol{d}$, which is obtained by premultiplying vector $\boldsymbol{m}$ by $\boldsymbol{S}^{-1}$:

$$\boldsymbol{d} = \boldsymbol{S}^{-1}\boldsymbol{m} \tag{4}$$

The following test statistics, have been shown to possess maximum power if $\boldsymbol{S}$ is a nondiagonal matrix (Mah & Tamhane, 1982):

$$Z^{\mathrm{MP}}_{d,j} = \frac{|d_j|}{\sqrt{W_{jj}}} \tag{5}$$

where $Z^{\mathrm{MP}}_{d,j}$ is the maximum power measurement test statistic for measurement j; d_j and W_{jj} are the elements of vector $\boldsymbol{d}$ and matrix $\boldsymbol{W}$, respectively. If the test statistic $Z^{\mathrm{MP}}_{d,j}$ is larger than the threshold values Z_{crit} (equal to 1.96 at level of confidence of 95%), then measurement j is declared to contain gross error. The expected value of $Z^{\mathrm{MP}}_{d,j}$, given by Eq. (6) (Bagajewicz, 2005a), is used:

$$E[Z^{\mathrm{MP}}_{d,j}] = \frac{\left|\sum_i W_{ji}\delta_i\right|}{\sqrt{W_{jj}}} \tag{6}$$

where δ_i is actual bias in measurement i.

Bagajewicz (2005a) used the maximum power measurement test to detect gross errors and determined the maximum undetected induced bias and thus obtained the software accuracy as defined using maximum undetected bias. This approach calculates the accuracy analytically but it represents the worse-case scenario and does not discuss the frequency of such scenario. To ameliorate the shortcomings of the analytical approach, we use a stochastic-based approach, which is presented next.

3. Stochastic-based accuracy

During the constant failure rate period of a sensor, the failure of the sensor is a random event. Each sensor has its own failure frequency which is independent of what happens with other sensors. Thus, at a specific point t in time, the induced bias and the accuracy is the function of the number, location and the sizes of undetected biases and also the number of eliminated measurements (so-called the state of the system). Therefore, the state of the system varies with time. A Monte Carlo simulation can be used to simulate failure event s of each sensor (within a specified time horizon) sampling the failure probabilities, which are obtained using sensor reliability data. When the conditions (e.g., failed or functioning) of all sensors in the system are available, the condition of the system is then obtained as a combination of the conditions of the individual sensors. Information on the condition of the system within a specified time horizon, obtained from the Monte Carlo simulation, is then used to calculate the accuracy; hence the name stochastic-based accuracy. Monte Carlo sampling procedure is described in next sections.

First note that after the sampling is performed, sensor failure times and also corrective actions are identified. Thus, in the

interval of time in between each of the failure times and/or corrective actions of all sensors, there is no change of the system, and therefore an accuracy value can be obtained using the real random values of the undetected biases in that interval. More precisely, accuracy value of estimator i within a time interval (t_s, t_{s+1}), $a_{i,(t_s,t_{s+1})}$, is calculated by:

$$a_{i,(t_s,t_{s+1})} = [\hat{\sigma}_i + \tilde{\delta}_i^{(p,n_T)}] = \hat{\sigma}_i + |([\boldsymbol{I} - \boldsymbol{SW}]\boldsymbol{\delta}_{n_T})_i| \quad (7)$$

where $\tilde{\delta}_i^{(p,n_T)}$ is the induced bias due to a specific set T of n_T undetected biases existing within the time interval (t_s, t_{s+1}), $\boldsymbol{\delta}_{n_T}$ the vector of bias sizes for the set T of n_T undetected biases and $\hat{\sigma}_i$ is the precision of estimator i. In case there is one or more measurements are eliminated, $\hat{\sigma}_i$ is replaced by $\hat{\sigma}_i^{\mathrm{R}}$, which is the residual precision after elimination of measurements.

The average value of accuracy within the time horizon T_{h}, $\bar{a}_i$, is calculated as the average value of all accuracy values in time intervals using the duration of the time intervals as weights.

$$\bar{a}_i = \sum_t \frac{a_{i,(t_s,t_{s+1})} \cdot (t_{s+1} - t_s)}{T_{\mathrm{h}}} \quad (8)$$

This average value $\bar{a}_i$ is also a random number. One Monte Carlo simulation attempt gives one value for $\bar{a}_i$. Finally, the expected value of accuracy of estimator i, $E[\hat{a}_i]$, is calculated as the mean value of $\bar{a}_i$ after N_{sim} simulations:

$$E[\hat{a}_i] = \frac{1}{N_{\mathrm{sim}}} \sum_{n=1}^{N_{\mathrm{sim}}} \bar{a}_{i,n} \quad (9)$$

where $\bar{a}_{i,n}$ is the average accuracy value obtained at simulation n.

Next, we briefly review the types of biases that can occur and then we present the Monte Carlo simulation procedure.

4. Types of biases

Biases in flow measurements can be attributed to many reasons including, but not limited to:

- Human faults: improper installation such as violation of upstream and downstream straight run requirement; improper calibration.
- Departure of operating conditions (temperature, pressure, density) from the standard conditions upon which meters are calibrated, or worse, operating outside the operation range of meters (for example, operating below the minimum Reynolds number requirement).
- Distortion of the flow profile at the measuring point due to entrainment of gas bubbles in the liquid stream, insufficient upstream and/or downstream straight run, erosion, corrosion, and particle deposits that change the roughness of the inside pipe surface.
- Sensor failure due to random events: we explain these in detail below.

Biases caused by the first three reasons can be mitigated by periodic sensor recalibration, and training skillful personnel so that sensors are properly installed and commissioned. On the other hand, sensor failures are usually invisible to operation personnel and the biases caused by usually go on undetected unless a gross error detection/data reconciliation system is in place.

We now focus our attention to biases that are caused by sensor failure. Three types of biases are considered:

(a) Sudden bias with fixed value (Fig. 1a). This can be described by a step function (positive or negative). The uncertainties are in the time at which the step takes place and the size of the bias. These are biases that typically emerge because of failures in electronic components (the readout system or the signal processing system) of the sensor. Generally, a sensor is prone to failure when fluid environment and/or ambient environment are harsh. For example, high ambient temperature, high humidity can cause damage to the electronic components. The local presence of power surges or the appearance of sudden electrical effects (e.g., lightening) may interfere with the readings and outputs of some meters (Endress Hauser FlowTec AG, 2004). Other events like the change in resistor impedance can cause a shift in output of the electric circuit.

(b) Randomly emerging drifts: these are characterized by ramps (up or down and not necessarily linear). The uncertainty is in the time at which the ramp starts and its slope or some parameter describing a non-linear drift. These are drifts attributable to wear and tear, deterioration of mechanical parts due to cavitations and sometimes to electronic failure. Some examples are wear and tear of bearing or turbine rotor in turbine meters, orifice plate in orifice meters. Once they appear, the wear and tear of sensor mechanical parts may continue until the part is damaged and the sensor stop working. The shape and slope of the drift are not known. We assume that the

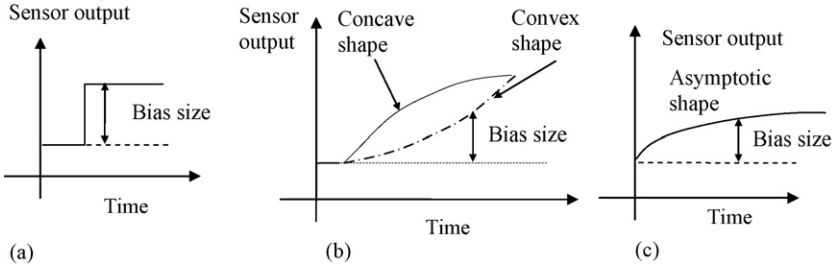

Fig. 1. Types of biases. (a) Bias type **a**: sudden bias with fixed value. (b) Bias type **b**: randomly emerging drifts. (c) Bias type **c**: deterministic drifts.

shape of randomly emerging drifts is either concave or convex as shown in Fig. 1b. We assume that the concave shape corresponds to biases caused by failures where the severity of failure initially increases rapidly with time and then slows down. An example of this type of failure is the corrosion of sensor parts that is gradually slowed down by a protective layer (which is in turn formed by the products of the corrosion process). We assume that the convex shape corresponds to biases caused by failures where the situation is opposite: the failure starts slowly and then speeds up. This usually occurs with mechanical failures like wear and tear, mechanical degradation. For the concave shape, we use a logarithmic function "bias size = $A \log(1 + (t/T))$" and for the convex shape is represented by an exponential function "bias size = $A (\exp(t/T) - 1)$", but other can be used. We ommit the linear relationship because is not usually the case in practice so it is disregarded.

(c) Deterministic drifts: these are not random events, but rather continuous processes that develop progressively with time, such as corrosion; coating, deposit of particles on sensor parts that are in contact with the fluid (the primary element of the sensor). If the fluid is corrosive and/or dirty, then one knows with high confidence that this type of bias exists, only parameters like the shape and slope of the drift being unknown. Corrosive/dirty fluids can damage or distort the shape and size of the sensor's primary elements which causes bias in measurement. The most common factor that affects the measurement accuracy is the coating or deposit of particles. Any amount of deposit may cause measurements to be in error; fortunately these are usually low for orifice plate meters (Upp & LaNasa, 2002). Generally, industrial fluids are not clean, and the fluids may get contaminated with lubricant, oil while passing through valves, compressors, pumps. They can also get contaminated with particles generated from erosion of metal pipes and fittings. The effects of this factor include: (i) changing the roughness of the pipe, which distorts flow profile, (ii) reduction in cross-section of flow, (iii) reduction of the mechanical clearances of moving parts, e.g., in turbine meter rotors, (iv) changing the original dimension of orifice plates, vortex bluff bodies, (v) insulation of electromagnetic meter electrodes, and (vi) blocking of pressure taps. Therefore, the dependence of bias size with time is usually a non-linear function because one single factor can cause multi effects that induce bias in the measurement. The shape and the slope of the drifts depend on the type of sensor and the nature of the problem that causes bias (drift). Particle deposits may reach an equilibrium where the number of particles deposited on the surface is equal to the number of particles on the surface layer swept away by the flowing fluid. In this case, the drifts have an asymptotic shape, as shown in Fig. 1c. Three *actual* cases of errors in measurement of orifice meters due to deposition of particles were discussed by Upp and LaNasa (2002), in which biases go on undetected for "a number of years". This implies that the drifts have asymptotic shape. Another cause of deterministic drift is corrosion, in which certain part of sensor that contacts with fluid may be continuously corroded until the sensor part is completely consumed and sensor stops working (drifts have opposite shape: concave shape) or the product of corrosion process (e.g., anhydrous iron oxides) may act as protective layer that slows down the corrosion process (drifts have asymptotic shape). We use the function "bias size = $A (1 - \exp(-t/T))$" to represent this asymptotic shape.

We further discuss in the appendix how these types of errors emerge in more detail. We also show there some typical values for the associated parameters.

5. Full Monte Carlo sampling approach

Our sampling procedure is the extension of the sampling procedure presented in Bagajewicz (2005a). The extensions are the following: (i) the bias size is sampled (it was not), (ii) different types of failures are considered (Bagajewicz considered only one), (iii) the dependence between measurements in gross errors detection is considered, and (iv) different strategies for plant data management are considered. The sampling procedure is described below.

For sensor failures that cause biases of type **a** (sudden occurrence with fixed value) and type **b** (randomly emerging drifts), the failure time is a random event. Moreover, with bias type **a**, the bias magnitude (A) is also a random number and is here assumed without loss of generality to follow a normal distribution $h_k(\theta_k, \bar{\delta}_k, \rho_k)$, but it can have any distribution without affecting the sampling procedure steps. For bias type **b**, the bias size increases continuously with time. The same thing is stated for the bias magnitude of deterministic drifts (bias type **c**). However, deterministic drifts appear right at the beginning when the sensor is put in use.

Next, the sampling procedure for bias type **a** (sudden occurrence with fixed value) is described: we assume that, at time $t = 0$, all sensors are as good as brand new. As time elapses, sensors may degrade and fail. Within the constant failure rate period of the bathtub curve, the failure of a sensor (sensor k) is a random event and its cumulative failure probability is given by (Bagajewicz, 2000):

$$f_k(t) = 1 - e^{-r_k t} \tag{10}$$

where r_k is failure rate of the sensor k.

To sample the time of failure, first we sample randomly the probability of failure $f_{k,1}(t)$ and calculate the failure time:

$$t = -\frac{1}{r_k} \ln(1 - f_{k,1}(t)) \tag{11}$$

We see that a sensor with higher failure rate will have shorter time to failure.

The next step is to sample the bias size according to its distribution (recall that, without loss of generality, we use a normal distribution). If the bias is large enough to be detected then the corresponding measurement is eliminated and the failed sensor is repaired (repair time is R_k). This sensor may fail again, so we sample the next failure of this sensor and the time from the

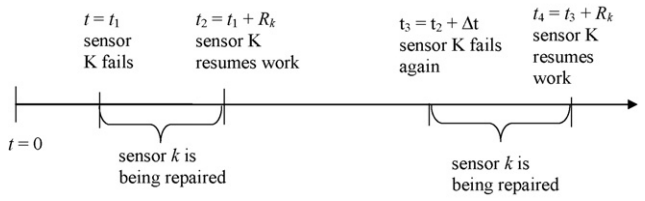

Fig. 2. Result of sampling two consecutive detected failures.

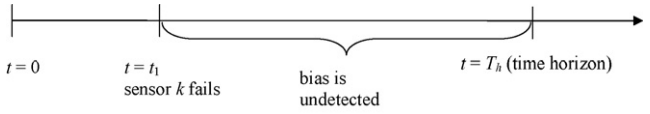

Fig. 3. Sampling of undetected failure.

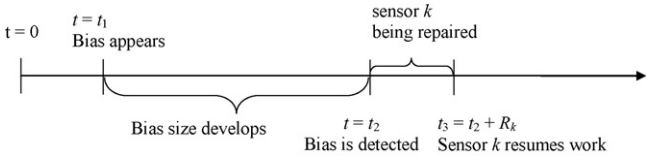

Fig. 4. Sampling of failure for randomly emerging drifts.

repair to the next failure is obtained. The magnitude of the bias is then sampled and if this bias is large enough to be detected, we have the situation depicted in Fig. 2.

If t_4 (Fig. 2) is still within the time horizon under consideration, we may have another failure, so we sample another failure time and bias size and so on. If a bias is undetected and if no preventive maintenance (that can detect hidden biases) is available, it continues undetected for the rest of the time horizon considered or until it is detected. This possibility is illustrated in Fig. 3.

Consider now a bias of type **b** (randomly emerging drifts). The time at which a bias appears is a random event. Because the size of the bias increases with time, the bias is eventually detected when the bias size reaches a threshold value. Then the sensor is repaired and resumes work. After that, we sample another failure of that sensor and the same cycle repeats. The described cycle is illustrated in Fig. 4.

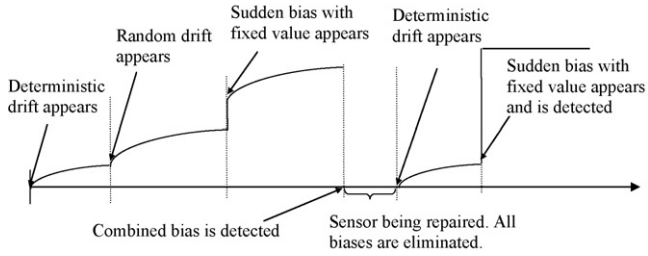

Fig. 5. Occurrence of three types of biases in a sensor.

With the deterministic drifts, the situation is almost the same as with randomly emerging drifts. The difference is that bias appears right at the beginning when the sensor is put into use.

After the sampling of failure events for all sensors has been performed, the condition of the sensors system is then obtained as the combination of the conditions of all the sensors. One example of such scenario is illustrated in Table 1 for a system with five sensors in which three sensors (sensors 1–3) are subjected to type **a** bias, one sensor (sensor 4) is subjected to type **b** bias and the last one (sensor 5) is subjected to type **c** bias.

The failure times and bias sizes for each kind of biases for each sensor are sampled separately and the overall bias is then calculated as combination of the three types of biases. When the bias is detected and sensor is repaired, we assume that the sensor is as good as brand new and samplings of the three types of biases are restarted in a new cycle. This situation is illustrated in Fig. 5.

Constructing the sample shown in Table 1 is complicated by the fact that the detection of a sensor failure is a function of the presence of biases in other sensors. Therefore, one cannot know if a sensor bias will be detected until all sensors are sampled. Take for example sensors 1 and 2 in Table 1. At times 12.2 and 54.8, respectively, these sensors develop a bias, which the table says are undetected. This is not known until all the other sensors are sampled. In turn, sensor 3 develops a bias and time 174.5, which is detected. When the original sampling was performed, it was not known that this bias would be detected. If it was not, then the bias would stay undetected until the end of the horizon. In

Table 1
Example of sampling results

Time (days)	0	12.2	54.8	174.5	177.5	318.9	365
Sensor 1	no bias	contains undetected bias S_1					
Sensor 2	no bias		contains undetected bias S_2				
Sensor 3	no bias			being repaired and measurement is eliminated	no bias	contains undetected bias S_3	
Sensor 4	no bias		contains undetected bias S_4 (bias size increases with time)				
Sensor 5	contains undetected bias S_5 (bias size increases with time)						
System condition	**contains S_5**	**contains S_1 & S_5**	**contains S_1 & S_2 & S_4 & S_5**	**contains S_1 & S_2 & S_4 & S_5 & one eliminated measurement**	**contains S_1 & S_2 & S_4 & S_5**	**contains S_1 & S_2 & S_3 & S_4 & S_5**	

such case, we do not perform a new sampling for the same type of failure. This is part of our simplifying assumptions: we do not consider a second failure of a sensor that has already failed. To do this, one would need to resort to a different reliability one that corresponds to an already failed sensor. Thus, to consider the interactions between biases in measurements, the sampling was conducted in the following way:

- Failure times and bias sizes for every sensor in the system are sampled and recorded until the end of time horizon is reached.
- The time intervals between failures in the system are obtained by combining the failure times of all sensors as illustrated in Table 1.
- At each failure time in the system, the maximum power measurement test (MPMT) is performed and the sensors that are detected being biased are singled out.
- If the MPMT cannot detect any bias, no action is needed. We then move on to investigate the next time interval until the end of time horizon is reached.
- If the MPMT flags the presence of biases, then, for each sensor with a detected bias a repair time is added and a new sampling for biases of types **a** and **b** is added. Type **c** bias is added if present.

The above procedure is somehow time consuming, because it requires marching through the time horizon and continuously re-sample the sensors whose failure has been detected. An alternative is to perform the first sampling and then apply the MPMT at fixed intervals ($t = 20, 40, 60, 80$, etc.). This reduces the number of times re-sampling is needed and it also reflects the fact that in practice, the gross errors detection (e.g., the measurement test) may be applied at periodic time intervals. We call the first case instantaneous testing and the second periodic testing. We compare both cases in the examples.

6. Examples

6.1. Example 1

Consider the example of Fig. 6, taken from Bagajewicz (2005b). Assume flowmeters with precision $\sigma_i^2 = 1$, 2 and 3, respectively. We also assume that the biases have zero mean and standard deviation $\rho_k = 2$, 4 and 6, respectively, failure rate of 0.025, 0.015, 0.005 (day^{-1}) and repair time of 0.5, 2 and 1 day, respectively. Although the example is very simple, it is used to point out the differences in methodology. The time horizon used was 5 years. The system is barely redundant: only one gross error can be determined, and when it is flagged by the measurement test, hardware inspection is needed to obtain its exact location. This is due to gross error equivalency (Bagajewicz and Jiang, 1998). The accuracy of estimator S_3 is calculated. We only consider the situation that only one type of bias can occur in a sensor, which is type **a** bias: sudden occurrence with fixed value to be able to meaningfully compare with earlier results (Bagajewicz, 2005b).

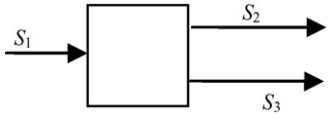

Fig. 6. Flowsheet for example 1.

We now illustrate the sampling procedure for these three sensors. In the MP measurement test, due to gross error equivalency, the test statistics for three measurements are the same, so if the test statistics are greater than threshold value, we assume that the measurement with biggest bias size is the detected one. Type **a** bias (sudden occurrence with fixed value) is considered and represented by a step change in sensor output as illustrated in Fig. 7. In this figure, the change (rather than absolute value) of sensor output (i.e. measurement) with time is depicted. The italic number right next to the step change is bias size. Fig. 7a shows the original sampling for the three sensors, indicating that at $t = 5.9$ the failure in sensor two (bias size = 5.4) was detected as being higher than the threshold (4.8).

Both biases in sensors one (taking place at $t = 8.9$) and sensor three (taking place at $t = 183.9$) are below their corresponding threshold values and are undetected. Fig. 7b shows the repair time and a new sampling for sensor two with a bias of 2.5 at $t = 156.1$. The error is again detected and therefore a new sampling is performed. Fig. 7c shows the corresponding repair time for sensor two and a third sampling for it. Note that the threshold value to detect a bias in sensor two without the presence of other biases is 4.8; it is due to interaction of biases that bias size of 2.5 (<4.8) in measurement two can still be detected. However, this observation cannot be generalized because it is possible that the threshold value for detecting biases is larger (not just smaller) due to interactions. Clearly, we see that if the biases in measurements 1, 2 (or 1, 3) are equal to each other, the MT test cannot detect biases whatever sizes they have. Now, after the second re-sampling of sensor two, the MP measurement test cannot detect any bias in the rest of the time horizon.

In turn, for periodic testing the sampling procedure exhibits some differences, as shown in Fig. 8. In this case, the original sampling is the same as in the case of instantaneous testing (Fig. 7a). Because the MPMT is conducted at a scheduled time in periodic testing, the bias in sensor two will be detected at the next scheduled time of MPMT after it appears, that is, at $t = 20$ (an interval time of 20 is used) as shown in Fig. 8b. This means that the undetected biases contribute to a worse accuracy than in the instantaneous testing, as one would expect. Fig. 8b shows the repair time of sensor two and a new sampling. Assuming the sampling had rendered the same numbers, one must observe that the new time for failure of sensor two is at $t = 170.2$ and the bias will be detected at $t = 180.0$, because of the regularity in testing. Although the same failure time samples as in instantaneous testing were used, the change is due to the fact that the sensor was now repaired at $t = 20$ and not at $t = 5.9$.

Because of the fact that testing is performed less frequently in periodic testing, we expect smaller computational time. This will be illustrated below.

The results of the average accuracy values are shown in Fig. 9 for 1000 sampling attempts and for both types of testing types. Table 2 shows that additional sampling does not alter

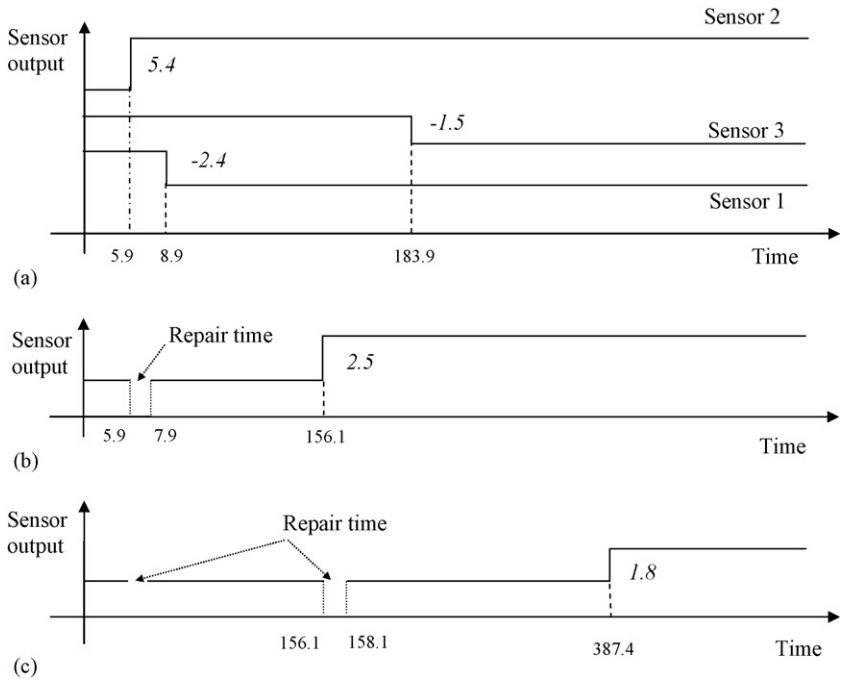

Fig. 7. Illustration of sampling procedure with instantaneous testing. (a) Original sampling. (b) Sensor two, first re-sampling. (c) Sensor two, second re-sampling.

significantly the result. Clearly we see that when number of sampling $N \geq 10^4$, the expected value of accuracy converges to a final solution of about 3.08. Comparatively, the accuracy value defined for maximum undetected bias of *one* bias present is 6.30 (Bagajewicz, 2005a, 2005b). This highlights the fact that using maximum undetected bias is too conservative.

In both cases, the lowest accuracy value obtained was around 1.23 (very near to the precision value of 1.225). The precision value is calculated as the square root of the corresponding diagonal element of the variance matrix of the estimators $\hat{\boldsymbol{S}}$, which is obtained by using the formula $\hat{\boldsymbol{S}} = \boldsymbol{S} - \boldsymbol{S}\boldsymbol{A}^{\mathrm{T}}(\boldsymbol{A}\boldsymbol{S}\boldsymbol{A}^{\mathrm{T}})^{-1}\boldsymbol{A}\boldsymbol{S}$ (Bagajewicz, 2000). The lowest value corresponds to the case where all biases are detected or undetected biases have very small sizes. The largest value observed was about 12.5 for instantaneous testing and 16.5 for periodic testing (these values are obtained after 10^6 simulations; hence they are not seen in Fig. 9).

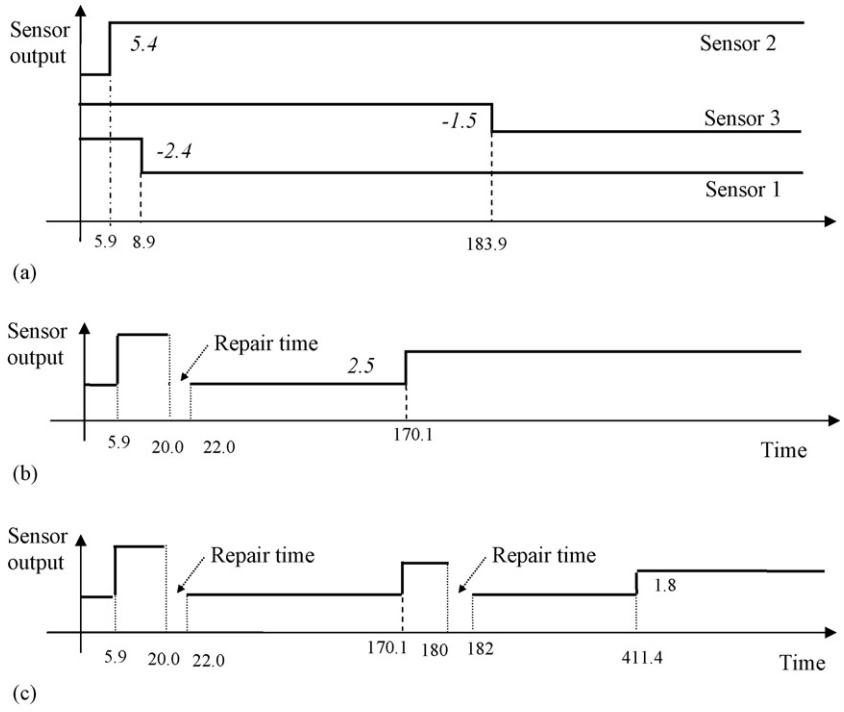

Fig. 8. Illustration of sampling procedure with periodic testing. (a) Original sampling. (b) Sensor two, first re-sampling. (c) Sensor two, second re-sampling.

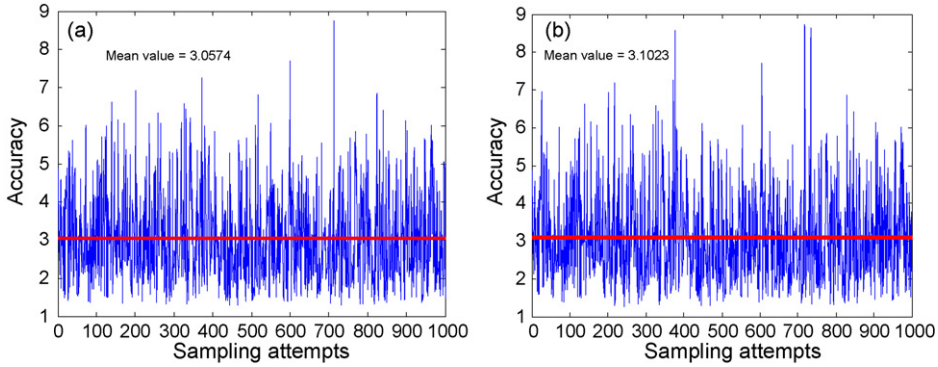

Fig. 9. Sampling accuracy results for example 1. (a) Instantaneous testing and (b) periodic testing.

These values correspond to the cases where almost all biases are undetected and the sizes of the biases are large. From Table 2, it is also obvious that, due to the delay in detecting the measurement biases of the periodic testing case, the expected value of accuracy obtained for periodic testing case is larger than the value obtained for instantaneous testing case.

In prior work (Bagajewicz, 2005b), the stochastic-based accuracy has been calculated to be 1.89, which is lower than the value we obtain here (3.08 and 3.13). The difference should not be attributed to the fact that a different time horizon was used (previous work used around 1 year). However, if a time horizon of 1 year is used, the expected value of accuracy is 2.40, which is still higher than the previously obtained value of 1.89. The difference is attributed to the fact that current work considers the interaction between biases leading to larger threshold values for detecting biases, which was not considered in previous work.

Consider now calculating the accuracy value at specific times, instead of calculating the average value of accuracy for the whole horizon. The results are shown in Fig. 10 (the number of samplings is 10^5). We see that, for small t, the sensors in the system are in good condition and few sensors fail. When time elapses, more and more sensors fail and that makes the accuracy worse (the accuracy value increases). This tells us that the stochastic accuracy is a function of time and therefore the real valuable tool is to know what is the expected value for different values of time, rather than one expected value over the whole (arbitrary) horizon. This information can be utilized in planning/scheduling the preventive maintenance activities to keep accuracy of estimators below certain values. This is possible because of the ability of preventive maintenance operations to detect all hidden biases so that the accuracy value returns back to normal value (i.e. precision value). For example, for the case of instantaneous testing, if we want to keep expected value of accuracy of estimator be lower than 2.7, it is necessary to perform preventive maintenance every 210 days (7 months).

Table 2
Expected value of accuracy if only corrective maintenance was used

Number of sampling	10^3	10^4	10^5	10^6
Expected value of accuracy				
Instantaneous testing	3.0574	3.0774	3.0752	3.0761
Periodic testing	3.1023	3.1308	3.1255	3.1303

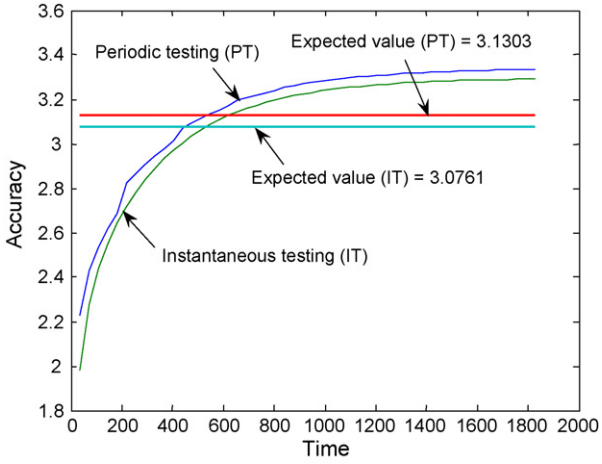

Fig. 10. Expected accuracy at specific points in time (corrective maintenance only).

Both the expected value over the whole time horizon and the value at a specific time of the instantaneous testing are smaller than the corresponding values of the periodic testing, as clearly depicted in Table 2 and Fig. 10. This is due to the delay in detecting biases of the periodic testing as explained above.

Another interesting feature to observe is the distribution of accuracy in any time interval. Figs. 11 and 12 show this distri-

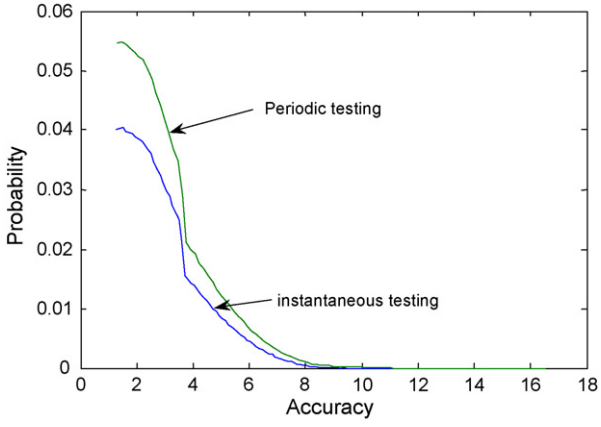

Fig. 11. Distribution of accuracy at time $t = 400$.

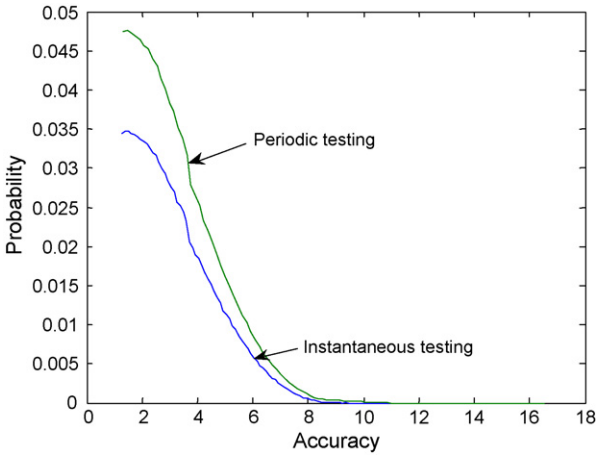

Fig. 12. Distribution of accuracy at time $t = 800$.

bution for accuracy at specific times $t = 400$ and 800 for both testing types.

The distribution of accuracy value at specific point in time is a monotonic decreasing function, that is, a small accuracy value has a higher probability than a large accuracy value. The probability that the system contains few biases with small bias sizes (i.e. small accuracy value) is larger than the probability that the system contains many biases with large bias sizes (i.e. large accuracy value) because the latter is the extreme case. As time increases, the distribution function shifts slightly to the right and the slope decreases, i.e. the probability for high accuracy value increases at the expense of lower probability for small accuracy value. As a consequence, the expected value of accuracy at a specific point in time increases when time increases. Fig. 10 confirms this result.

Fig. 13 shows the distribution of the accuracy obtained for the whole time horizon (the average value $\bar{a}_i$).

The distribution of the average accuracy value is a combination of distributions of the accuracy values in all time intervals within the time horizon (that shift to the right as time increases). Fig. 13 shows that, unlike the monotonic decreasing distribution function of accuracy at a time or in a time interval, the

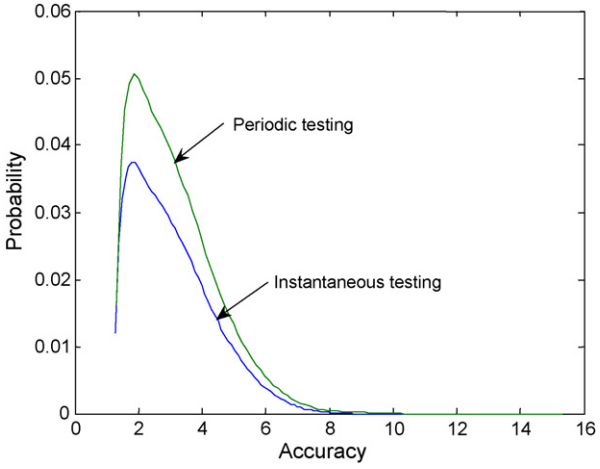

Fig. 13. Distribution of all average accuracy.

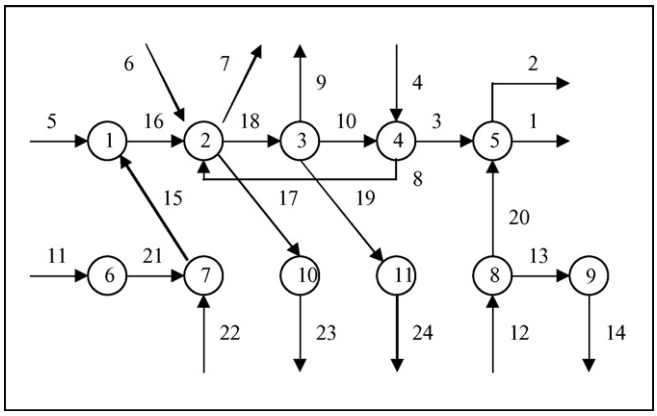

Fig. 14. Example 2.

distribution of the average accuracy exhibits a peak. This can be explained by the fact that low accuracy values in the left hand side of the peak have low probability at the end of time horizon while high accuracy values in the right hand side of the peak have low probability in the whole time horizon. The expected value of accuracy is slightly to the right of this peak because the distribution function has a rather long tail on the right side.

6.2. Example 2

Consider one large scale example process as illustrated in Fig. 14 (taken from Bagajewicz, 2000). Assume that all streams are measured with the flowrates given in Table 3.

The parameters for the sensors are:

- Precision = 2.5% (for all sensors).
- Failure rate: $r_i = 0.01$ (day^{-1}), $i = 1, 3, 5, \ldots, 23$ and $r_i = 0.02$ (day^{-1}), $i = 2, 4, 6, \ldots, 24$.
- Repair time $R_i = 1$ day, $i = 1, 3, 5, \ldots, 23$ and $R_i = 2$ days, $i = 2, 4, 6, \ldots, 24$.

No information regarding the slope of deterministic drifts and the shape and slope of randomly emerging drifts is available, so we made some reasonable assumptions. The deterministic drifts with asymptotic shape is represented by the following expression: bias size $= A(1 - \exp(-t/T))$, with $A = 10$, $T = 500$. The randomly emerging drifts with assumed concave shape are represented by the following expression: bias size $= A \ln(1 + (t/T))$ with $A = 10$, $T = 200$. With these assumed parameters and when

Table 3
Flow rates for example 2

Stream	Flow	Stream	Flow	Stream	Flow
S_1	140	S_9	10	S_{17}	5
S_2	20	S_{10}	100	S_{18}	135
S_3	130	S_{11}	80	S_{19}	45
S_4	40	S_{12}	40	S_{20}	30
S_5	10	S_{13}	10	S_{21}	80
S_6	45	S_{14}	10	S_{22}	10
S_7	15	S_{15}	90	S_{23}	5
S_8	10	S_{16}	100	S_{24}	45

Table 4
Calculated results for example 2 for precision and accuracy of estimators, type **a** bias

Streams	$\hat{\sigma}$ (%)	$\hat{a}$ (%)		Streams	$\hat{\sigma}$ (%)	$\hat{a}$ (%)	
		Instantaneous testing	Periodic testing			Instantaneous testing	Periodic testing
S_1	1.6884	2.8109	3.0014	S_{13}	0.3063	0.9428	3.8035
S_2	1.2294	8.8902	9.8368	S_{14}	0.3063	1.0200	3.6143
S_3	1.5091	2.5469	2.6360	S_{15}	1.0464	2.1050	2.2527
S_4	0.2148	5.5509	5.8236	S_{16}	0.9587	2.0303	2.2585
S_5	0.6155	8.1772	10.3344	S_{17}	0.1560	0.3961	4.8334
S_6	2.1771	4.6975	5.4101	S_{18}	1.0519	2.0774	2.2811
S_7	0.9140	7.4757	9.4115	S_{19}	1.2604	2.5965	2.9082
S_8	0.6186	12.0797	14.0775	S_{20}	1.1841	3.0677	3.8595
S_9	0.6186	10.1913	11.2757	S_{21}	1.1827	2.2447	2.4238
S_{10}	1.5437	2.8862	3.0635	S_{22}	0.6147	10.0520	11.9800
S_{11}	1.1827	2.2008	2.4224	S_{23}	0.1560	0.4145	4.8414
S_{12}	0.9109	2.2631	2.9961	S_{24}	1.2604	2.5326	2.9184

Table 5
Calculated results for example 2 for precision and accuracy of estimators, type **b** bias

Streams	$\hat{\sigma}$ (%)	$\hat{a}$ (%)		Streams	$\hat{\sigma}$ (%)	$\hat{a}$ (%)	
		Instantaneous testing	Periodic testing			Instantaneous testing	Periodic testing
S_1	1.6884	3.0962	2.9851	S_{13}	0.3063	0.4449	1.2907
S_2	1.2294	19.5075	20.1140	S_{14}	0.3063	0.4465	1.3017
S_3	1.5091	2.2896	2.5873	S_{15}	1.0464	1.8459	2.1185
S_4	2.2148	3.9792	4.2165	S_{16}	0.9587	2.1101	2.6849
S_5	0.6155	9.3501	13.4592	S_{17}	0.1560	0.2005	11.4142
S_6	2.1771	3.4704	4.0080	S_{18}	1.0519	3.3920	3.6653
S_7	0.9140	5.3737	8.8483	S_{19}	1.2604	2.0467	2.5651
S_8	0.6186	31.7520	31.7850	S_{20}	1.1841	7.2310	10.1793
S_9	0.6186	5.0263	7.2162	S_{21}	1.1827	3.4997	4.3318
S_{10}	1.5437	4.8755	5.1889	S_{22}	0.6147	17.6672	22.0316
S_{11}	1.1827	3.4272	4.1994	S_{23}	0.1560	0.1998	10.0612
S_{12}	0.9109	5.7756	7.9555	S_{24}	1.2604	2.0286	2.5439

no other biases interfere with the detection of the drifts, usually the drifts will be detected around 1 year (for deterministic drifts) and 3 month (for randomly emerging drifts) after they start, which are reasonable numbers. The number of sampling attempts is 1000, time horizon is 365 (days). If only corrective maintenance is applied, the results of Tables 4–6 were obtained. Table 4 shows the results when only type **a** biases are included.

We see that some estimators are highly vulnerable to undetected biases in the system. Indeed, the estimators of streams S_8, S_9 have an accuracy value about 20 times more than their precision value (accuracy without biases). Usually this problem applies to the estimators of low flowrates. On the other hand, some estimators are not very sensitive to the presence of undetected biases such as estimators of streams S_1, S_3 where accuracy

Table 6
Calculated results example 2 for precision and accuracy of estimators, type **c** bias

Streams	$\hat{\sigma}$ (%)	$\hat{a}$ (%)		Streams	$\hat{\sigma}$ (%)	$\hat{a}$ (%)	
		Instantaneous testing	Periodic testing			Instantaneous testing	Periodic testing
S_1	1.6884	2.4301	2.4457	S_{13}	0.3063	0.3907	2.3787
S_2	1.2294	14.4466	14.5100	S_{14}	0.3063	0.3907	2.3787
S_3	1.5091	2.4575	2.4701	S_{15}	1.0464	3.0243	2.9454
S_4	2.2148	4.8314	3.8108	S_{16}	0.9587	5.3227	5.2581
S_5	0.6155	26.4296	26.5137	S_{17}	0.1560	51.5232	51.6569
S_6	2.1771	3.2488	3.3620	S_{18}	1.0519	3.3369	3.2887
S_7	0.9140	17.2913	17.2935	S_{19}	1.2604	5.2672	5.1392
S_8	0.6186	26.2209	26.2938	S_{20}	1.1841	9.4377	9.4118
S_9	0.6186	25.8675	25.9056	S_{21}	1.1827	5.0940	5.1731
S_{10}	1.5437	5.3859	5.3585	S_{22}	0.6147	14.3027	15.6376
S_{11}	1.1827	5.0940	5.1731	S_{23}	0.1560	51.5232	51.6569
S_{12}	0.9109	7.1062	7.1306	S_{24}	1.2604	5.2675	5.1394

value is just 2 times more than precision value. The estimators of these streams are said to be more robust to the presence of undetected biases. Usually the estimators of high flowrates exhibit this characteristic. The reason is that, with high flowrates, the induced bias is relatively small when compared with the flowrate value, which is not the case for small flowrates where induced bias can be many times larger than the flowrate value. Moreover, because low flowrates are sensitive to undetected biases, they are also sensitive to the delay in the detection of biases as can be seen in estimators of streams S_{13}, S_{14}, S_{17} whose accuracy for the case periodic testing are much larger than the accuracy for the case instantaneous testing.

In turn, Table 5 shows the results when only type **b** biases are considered.

The results in Table 5 show that, generally, accuracy values of estimators for type **b** biases are comparable to those values for type **a** biases because, in essence, type **b** biases are somewhat similar to type **a** biases in the sense that bias occurrence is random for both of them.

Next, Table 6 shows the results when only type **c** biases are considered.

With biases type **c**, the biases appear right after sensors are put into use. The biases keep undetected until their sizes reach threshold values. The biases are then identified and sensors are repaired. When sensors resume work, biases appear again and the same cycle repeats. The presence of this type of bias is possible if the fluid is highly corrosive, dirty such that it affects the sensors right after sensors are put into use. This means that the measurements always contain undetected biases so it is expected that the accuracy values for type **c** biases (shown in Table 6) are worse (larger) than the accuracy values for biases types **a** and **b** (shown in Table 4 and 5), which is shown to be true by calculation results.

Finally, consider the case that three types of biases can occur in a sensor (all sensors contain simultaneously three types of biases), the same parameters for three kinds of biases as stated above are used and the calculated results are given in Table 7.

The calculations show that the accuracy value obtained when three types of biases can occur in a sensor (Table 7) is larger than the accuracy value when only one type of bias of types **a** or **b** is present (Tables 4 and 5). This is due to the fact that more types of biases that can occur in a sensor lead to a larger chance for the sensor to be biased, thus the accuracy value increases. Considering two cases, this case (all three biases, Table 7) and the case that only type **c** bias is present (Table 6): in both cases the measurement sets always contain some undetected biases. Type **c** bias is always present in measurement, other types of biases (**a** and **b**) may add up to increase the type **c** bias size (total bias size > type **c** bias size), or contrarily it reduces the type **c** bias size (cancellation effect). So there is no way to say a priori, which one renders better accuracy, as seen from Tables 6 and 7. Finally note that the failure rate is determined experimentally and only one value is reported, so there is no such specific failure rate data available associated with a specific failure mechanism (i.e. specific type of bias). However, one can assume that the failure rates for all types of biases that occur suddenly (types **a** and **b** bias) are the same, which is the assumption used in our calculation.

Table 8
Comparison of computation time for the two cases

Computation of accuracy value in the case of	Instantaneous testing	Periodic testing
Type **a** bias only	46 min 42 s	31 min 18 s
Type **b** bias only	3 h 20 min 16 s	46 min 20 s
Type **c** bias only	2 h 36 min 13 s	44 min 27 s
All three types of biases occurring	11 h 10 min 35 s	1 h 20 min 10 s

Table 8 shows the computation time for the two cases: instantaneous testing and periodic testing. It is clear that the computation time of the former is much longer than that of the latter because the former requires more computation as explained above.

7. Recommendations

The calculated accuracy value is dependent of various factors discussed in this paper: the type of bias of the sensor and the data management policy in the process plants (i.e. instantaneous testing or periodic testing). The accuracy value should be calcu-

Table 7
Calculated results for precision and accuracy of estimators, simultaneous occurrence of three types of biases

Streams	$\hat{\sigma}$ (%)	$\hat{a}$ (%)		Streams	$\hat{\sigma}$ (%)	$\hat{a}$ (%)	
		Instantaneous testing	Periodic testing			Instantaneous testing	Periodic testing
S_1	1.6884	4.9093	4.4863	S_{13}	0.3063	2.2078	11.4764
S_2	1.2294	30.1158	37.8656	S_{14}	0.3063	2.2032	11.5099
S_3	1.5091	3.4455	4.7932	S_{15}	1.0464	2.7115	3.7162
S_4	2.2148	6.6107	9.1013	S_{16}	0.9587	2.9667	6.2045
S_5	0.6155	15.3902	46.8299	S_{17}	0.1560	4.9375	23.1131
S_6	2.1771	4.8178	8.5218	S_{18}	1.0519	4.0597	6.4346
S_7	0.9140	16.7190	40.2522	S_{19}	1.2604	3.0115	7.7386
S_8	0.6186	32.3781	56.9956	S_{20}	1.1841	4.3948	10.8835
S_9	0.6186	13.3956	35.4492	S_{21}	1.1827	3.9535	7.0445
S_{10}	1.5437	5.5240	8.9567	S_{22}	0.6147	19.4882	39.7981
S_{11}	1.1827	3.9125	6.9407	S_{23}	0.1560	5.0998	22.6615
S_{12}	0.9109	3.2366	8.6515	S_{24}	1.2604	2.9820	7.5920

lated using the best knowledge about such factors. Information on the data management policy is readily available. If one does not know for certain about the type of bias that might occur, it is recommended that the (sudden) occurrence of only type **a** bias or type **b** bias is used because this is the most common and likely case.

8. Conclusions

The stochastic-based approach to calculate the accuracy is realistic because it reflects the random nature of failure events of sensors in the system. Moreover, it also reflects the different frequencies of failure of different sensors. This approach can also be used to obtain the expected accuracy through time. As time elapses, more and more sensors fails and accuracy value increases. This information can be utilized in planning/scheduling preventive maintenance activities to preserve equipment function and improve measurement accuracy.

It has also been shown that some measurements are highly vulnerable to the presence of undetected biases where induced biases are larger than the standard deviation (i.e. precision) many times (the underlying assumption is that data reconciliation is used).

Three types of biases have been investigated separately and also in combination (simultaneous occurrence of the three types of biases). The results show that the type **a** bias (sudden occurrence with fixed value) has the least effect on the value of accuracy, while type **c** bias (deterministic drifts) and the combination of biases have the most effect on accuracy value.

Appendix A. Failure modes of flowmeters

A.1. Differential pressure flowmeters

Differential pressure meters are the most commonly used flowmeters. Their operation is based on the premise that the pressure drop across the meters is proportional to square of the volumetric flowrate. Like most flowmeters, differential pressure flowmeters have a primary and secondary element. The primary element causes a constriction in the flow cross-section area to create change in pressure. The secondary element measures the differential pressure and provides the signal or read-out that is converted to the actual flow value (Miller, 1996).

Different kinds of differential pressure flowmeters are characterized by how the flow cross-section area is constricted. In the orifice flowmeter, the most popular liquid flowmeter in use today, the flow cross-section area is suddenly restricted by making use of an orifice plate. In a Ventury flowmeter, the pipe diameter is gradually constricted. Other differential pressure flowmeters are flow nozzles, pitot tubes, flow tubes, and elbow meters (Fig. A1, taken from Analog Devices Inc., 2005).

Failure modes involving mechanical parts of the meters include erosion, corrosion, deposit of particles due to dirty and/or corrosive fluids, leak through the flanges at the orifice plates, cavitation damage, plugging of pressure taps (Padmanabhan, 2000; Taylor, 1994). Failure modes involving

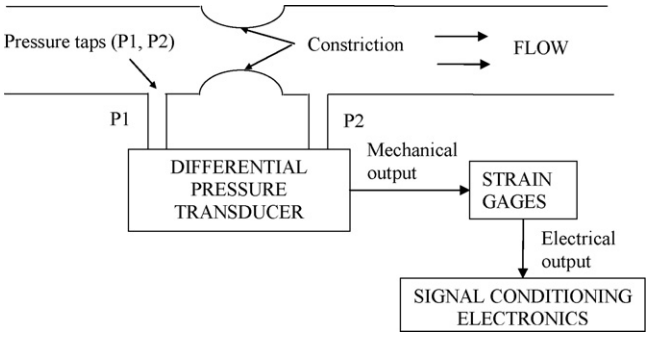

Fig. A1. Simplified structure of differential pressure flowmeters.

the electronic parts or the transmitters (for signal amplification, linearization, etc.), include complete stoppage or step change in the output signal which is usually caused by harsh ambient conditions or significant change in ambient environment; the failure rate of electronic parts, however, is smaller than that of the mechanical parts. Failures involving electronic parts occur suddenly and the measurement bias develops in a step-wise fashion. Conversely, failures involving mechanical parts occur gradually and, consequently, the bias size increases gradually with time. The failure rates of differential pressure flowmeters for measuring liquid flow are given in Table A1 (Taylor, 1994).

Different kinds of (simulated) failure modes and their associated measurement errors of orifice flowmeters were studied by the Florida Gas Transmission Company (McMillan & Considine, 1999). Some results of that study are given in Table A2.

Three *actual* cases of errors in measurement of orifice meters due to deposition of particles were discussed by Upp and LaNasa (2002). The meters were measuring from 1 to 3% lower than the unbiased values and the biases went on undetected for "a number of years".

A.2. Mechanical flowmeters

Mechanical flowmeters measure flow making use of moving parts (rotors), either by delivering isolated, known volumes of fluid through champers (positive displacement meters) or by recording the rotational speed of rotor as function of fluid velocity (turbine flowmeters). Positive displacement meters operate by isolating and counting a known volume of fluid while moving. The turbine flowmeter, a velocity meter, con-

Table A1
Failure rate of differential pressure flowmeters (Taylor, 1994)

Failure mode	Failure rate
Mechanical parts faults (for liquid flow)	
Drift greater than 5% from calibration	$5/10^6$ h
No output signal	$4/10^6$ h
Output signal high	$1/10^6$ h
Transmitter fault	
Short circuit/no signal	$0.5/10^6$ h
Fail high signal/short circuit	$0.2/10^6$ h
Drift greater than 5%	$1/10^6$ h

Table A2
Failure modes and their associated measurement errors of orifice flowmeters

Condition	%Error
Orifice edge beveled 45° circumference	
0.01 bevel width	−2.2
0.02 bevel width	−4.5
0.05 bevel width	−13.1
Turbulent gas stream (distortion of flow profile) due to	
Upstream valve partially closed	−6.7
Grease and dirt deposits in meter tube	−11.1
Leak around orifice plate	
1. One clean cut through plate sealing unit	
a. Cut on top side of plate	−3.3
b. Cut next to tap holes	−6.1
2. Orifice plate carrier raised approximately 3/8 in. from bottom (plate not centered)	−8.2
Valve lubrication on upstream side of plate	
Bottom half of plate coated 1/16 in. thick	−9.7
Three gob-type random deposits	0.0
Nine gob-type random deposits	−0.6
Orifice plate uniformly coated 1/16 in. over full face	−15.8
Valve lubrication on both sides of plate	
Plate coated 1/8 in. both sides of full face	−17.9
Plate coated 1/4 in. both sides full face	−24.4

sists of a multiple-bladed rotor perpendicular to the fluid flow. The rotor spins as the liquid passes through the blades. The rotational speed is a direct function of flow velocity and can be sensed by a magnetic pick-up or a photoelectric cell.

It is well known that the moving parts are the weakest link in the structure of the meters. The rotor and the bearing will be eventually damaged due to abrasion, corrosion, wear and tear, especially when exposed to dirty, corrosive fluid and this problem causes bias in measurement. Under certain conditions, the pressure drop across the turbine meters can cause flashing, which in turn causes the meters to read high or cavitation, which results in rotor damage (Omega Engineering Inc., 2005; Padmanabhan, 2000). The failure rate of these mechanical meters is comparable to that of positive displacement pumps which is 30–60/10^6 h (Taylor, 1994). As in the case of orifice plates, we also consider the possibility of sudden emergence of a steady bias, or drifts due to slow mechanical wear and tear.

A.3. Other flowmeters

- *Electromagnetic meters* operate on Faraday's law of electromagnetic induction, which states that a voltage will be induced when a conductor moves through a magnetic field. The liquid serves as the conductor; the magnetic field is created by energized coils outside the flow tube. A pair of electrodes penetrates through the pipe and its lining to measure the amount of voltage produced, which is directly proportional to the velocity of fluid.
- *Vortex meters* make use of a natural phenomenon that occurs when a liquid flows around a bluff object. Eddies or vortices are shed alternately downstream of the object. Piezoelectric or capacitance-type sensors (located either inside or outside the meter body) are used to detect the frequency of the vortex shedding which is directly proportional to the liquid velocity.
- *Ultrasonic meters* operate on the principle that the speed at which the sound propagates in the liquid is dependent on the fluid's density. If the fluid's density is constant, one can use the time of ultrasonic passage (or reflection) to determine the velocity of the flowing fluid. The ultrasonic meters consist of two transducers: one to transmit the ultrasonic signal, one to receive the ultrasonic signal that pass through the fluid or is reflected when contacted with discontinuities (e.g., particles) in the fluid.
- *Coriolis meters* are based on diverting the flow through a small tubing and measuring the Coriolis force exerted as the fluid turns inside the tube.

Having no moving parts, and being relatively non-intrusive (that is, they do not directly contact or obstruct fluid flow), these meters are considered to be reliable, that is, with lower failure rate than orifice and turbine meters. The common failure mode for these advanced meters is the erosion of the coating of the electrodes in electromagnetic meters or the erosion in the coating of the inside surface of the pipe. This erosion leads to a loss in stimulus force (e.g., magnetic field in electromagnetic meters) and/or the output signal and consequently, it affects the accuracy of meters. Finally, the erosion of the coating of the bluff body in vortex meters changes its dimensions (Omega Engineering Inc., 2005; Padmanabhan, 2000) and therefore affects accuracy. Moreover, because these meters make use of sophisticated electronics technology, failure of signal conditioning electronic parts also needs to be considered.

References

Analog Devices Inc. (2005). *Practical design techniques for sensor signal conditioning* (accessed in 2005, available at http://www.analog.com).

Bagajewicz, M., & Jiang, Q. (1998). Gross error modeling and detection in plant linear dynamic reconciliation. *Computers and Chemical Engineering*, *22*(12), 1789–1810.

Bagajewicz, M. (2000). *Design and upgrade of process plant instrumentation*. Lancaster, PA: Technomic Publishers.

Bagajewicz, M. (2005a). On the definition of software accuracy in redundant measurement systems. *AIChE Journal*, *51*(4), 1201–1206.

Bagajewicz, M. (2005b). On a new definition of a stochastic-based accuracy concept of data reconciliation-based estimators. In *European Symposium on Computer-Aided Process Engineering Proceeding (ESCAPE)*

Endress Hauser FlowTec AG. (2004). *Flow handbook* (2nd ed.).

Mah, R. S. H., & Tamhane, A. C. (1982). Detection of gross errors in process data. *AIChE Journal*, *28*, 828–830.

McMillan, G. K., & Considine, D. M. (1999). *Process industrial instruments and controls handbook* (5th ed.). New York: McGraw-Hill.

Miller, R. W. (1996). *Flow measurement engineering handbook*. New York: McGraw-Hill.

Omega Engineering Inc. (2005). *Transactions in measurement and control, Vol. 4* (accessed in 2005, available at http://www.omega.com).

Padmanabhan, T. R. (2000). *Industrial instrumentation: principles and design*. London: Springer-Verlag.

Taylor, J. R. (1994). *Risk analysis for process plant, pipelines and transport*. London: E & FN Spon.

Upp, E. L., & LaNasa, P. J. (2002). *Fluid flow measurement* (2nd ed.). Boston: Gulf Professional Publishing.